Ionospheric effects on synthetic aperture radar (SAR) clutter statistics

Belcher, David P.; Cannon, Paul S.

[Link to publication on Research at Birmingham portal](#)

Ionospheric effects on synthetic aperture radar (SAR) clutter statistics

David P. Belcher, Paul S. Cannon

EE&CE, University of Birmingham, Edgbaston, Birmingham B15 2TT, UK
E-mail: d.belcher@bham.ac.uk

Abstract: Low-frequency space-based synthetic aperture radar (SAR) is an ideal sensor for measuring forest biomass, but can suffer from ionospheric effects. The variation in total electron content (TEC), originating from ionospheric turbulence, causes the along track point spread function (PSF) to degrade in a manner which depends on ionospheric conditions. In this study, the effect of this PSF on the single point statistics (probability density function) and two point statistics (autocorrelation function (ACF)) is derived. It is shown that the K-distribution order parameter is directly proportional to the ionospheric turbulence, as quantified by C_kL. The complex ACF is a measure of amplitude scintillation, and the intensity ACF is a measure of both the order parameter and the terrain correlation length. A simulation is performed which clearly shows that measuring the order parameter ratio between ionospherically disturbed and undisturbed images is a measure of C_kL. This measure can be used two orders of magnitude below the point where the ionosphere causes defocusing of the SAR image. It is concluded that the usefulness of this new measure can only be verified by experimental data since the temporal stability of the underlying order parameter is unknown.

1 Introduction

1.1 Background

Space-based synthetic aperture radar (SAR) is a useful remote sensing tool, being relatively unaffected by tropospheric weather. A promising application for space-borne SAR is the measurement of the Earth's forest biomass, an important parameter for accurate prediction of global climate change. However, this requires a low-frequency SAR (1 GHz and below) with foliage penetration characteristics that result in a backscatter that depends on the volumetric vegetation. Unfortunately, at low frequencies the radar signal is affected by the ionosphere, which is an important limiting factor [1].

The main effect of the ionosphere is to perturb the phase of an RF signal, the size of the effect being determined by both the RF frequency and by the total electron content (TEC) experienced by a signal passing through it. This phase perturbation manifests itself in a variety of ways in the SAR image, resulting in Faraday rotation, a time delay that causes image shift, and defocusing in both the range and azimuth directions. The range defocusing, if any, can easily be corrected [1] but the along track azimuthal defocusing is much harder to remove because it is the result of variations in TEC along the satellite track. It can be shown that this produces a point spread function (PSF) with a characteristic shape, whose form can be derived analytically [2, 3].

In this paper, the effect of the ionosphere on the SAR clutter statistics is considered using the known form of the PSF. In the rest of Section 1, the nature of the ionospheric effect on SAR will be reviewed, and the effect on clutter considered. In Section 2, the effect on the single point statistics is derived, and it is shown that although the contrast is not a useful measure of the ionosphere, the change in the order parameter is directly related to the ionospheric turbulence, as quantified by C_kL. In Section 3, the two point statistics are considered, and it is shown that the complex autocorrelation function (ACF) is a measure of the amplitude scintillation, whereas the intensity ACF can be used to measure both the order parameter and determine the terrain correlation length. Simulations to test the theory are conducted in Section 4 and conclusions are drawn in Section 5.

1.2 Ionospheric propagation

The simplest model of ionospheric propagation is that of geometric optics, in which a straight line ray path is propagated from the satellite, penetrates the ionosphere at the ionospheric penetration point (IPP) and then propagates onwards to impinge on a ground target. The radar pulse is then reflected back through the ionosphere before being received back at the radar. In this model the ionosphere is often considered to be a thin two-dimensional phase screen, generally placed close to the F-region electron density peak. For low Earth orbiting SARs, this is approximately half way between the satellite and the ground.

When electromagnetic radiation propagates through the ionosphere, it experiences a phase advance, which in the high frequency limit (100 MHz and above in the Earth's

ionosphere) is equal to $r_e\lambda\text{TEC}$ where r_e is the classical electron radius, λ is the wavelength and the TEC is measured along a one way ray path. The effects of this frequency dependent phase advance on the radar pulse as a whole are, in order of decreasing importance, to phase shift, delay and defocus it. [1]

Although the constant TEC effects of the ionosphere on a sequence of pulses can be ignored or corrected, there remains a phase shift which will vary from one radar pulse to the next. This is because the phase shift is very sensitive to small variations in TEC. Since the turbulent ionosphere consists of many randomly distributed irregularities in electron density, the central limit theorem can be invoked, so that after removing average TEC effects (which can be considered constant over a synthetic aperture) all that remains is a zero mean Gaussian distributed phase term

$$\delta\psi = -2r_e\lambda_0\delta\text{TEC} \qquad (1)$$

where λ_0 is the centre wavelength of the radar pulse. Provided that the standard deviation of $\delta\psi$ over a synthetic aperture is less than $\pi/4$ (so that 95% of the phase values lie within 0 to π) the SAR image will not experience significant loss of resolution. However, the phase modulation $\delta\psi$ will still affect the shape of the PSF in the SAR image [3].

The thin phase screen model is inherently multiplicative because it multiplies the signal passing through it at the IPP, and is appropriate under weak scattering conditions. The signal modulation (known as scintillation) can include the effects of diffraction on amplitude scintillation by further extending the model [4–6].

As the standard deviation of the phase $\delta\psi$ becomes larger, the phase cannot be modelled by a thin phase screen but can be modelled as a thick phase screen. This occurs when the standard deviation of the phase exceeds 2π, at which point the phase modulo 2π becomes almost uniformly distributed. At this point, the central limit theorem can again be invoked so that the signal is composed of two independent Gaussian distributions in real and imaginary components. Such large variations also scatter the radar signal so that scattering from nearby regions of the ionosphere, away from the line-of-sight, contribute to the received signal. This is the strong scattering regime, and such a signal cannot be focussed by a SAR and is best considered as additive noise [7] or as multiple thick phase screens.

In this paper, the multiplicative thin phase screen model will be assumed, rather than the additive noise model and the effects on the SAR clutter statistics derived accordingly.

1.3 Point spread function

The SAR image is generated by Fourier transformation over the synthetic aperture of the received signal reflected from ground targets. After the usual SAR processing and matched filter have been applied, this can be represented by

$$F\{A(x)\exp[i\psi(x)]\} = h(x) \qquad (2)$$

where $F\{\ \}$ denotes Fourier transformation, $A(x)$ is the amplitude weighting over the synthetic aperture, x is the distance along the synthetic aperture or image and $\psi(x)$ is the phase modulation over the aperture because of the ionosphere. If there are no ionospheric effects on the SAR, $\psi(x) = 0$, and the SAR PSF $h(x)$ is given by the Fourier transform of the weighting function $A(x)$. Thus, for a

uniform weighting, that is, $A(x) = 1/L_{SA}$, the PSF will be $\text{sinc}(\pi x L_{SA})$ where L_{SA} is the length of synthetic aperture. In general, a reasonable amplitude weighting function will be chosen [8] so as to create a delta-like PSF in the absence of ionospheric effects.

Since the phase modulation is small for weak scattering, $\exp[i\psi(x)] \simeq 1 + i\psi(x)$ and the PSF can be approximated to the sum of a mainlobe plus sidelobes [3]

$$h(x) \simeq F\{A(x)\} + iF\{\psi(x)\} \qquad (3)$$

where the mainlobe is given by $F\{A(x)\}$ and the sidelobes are given by $F\{\psi(x)\}$. It has also been assumed that the effect of the amplitude weighting on the sidelobes can be approximated to a convolution with a delta function. The sidelobe function (SLF), as given by $F\{\psi(x)\}$, can be related to the phase power spectrum in the phase screen [2, 3], which has a power law form, and consequently the sidelobe shape is given by

$$\langle|\text{SLF}(r)|^2\rangle = T_{SLF}\left(\sqrt{r_0^2 + r^2}\right)^{-p} \qquad (4)$$

where r is the distance in the SAR image, measured in resolution cells from the mainlobe peak, p is the spectral slope of the phase screen power law and $r_0 = L_C/l_0$ is the ratio of the coherence length in the phase screen to the ionosphere's outer scale size l_0. The form of the image SLF above is the ensemble average power spectrum, as denoted by $\langle\ \rangle$. Each realisation of the sidelobes will have a random phase and amplitude. The constant of proportionality is given by Belcher and Rogers [3]

$$T_{SLF} = 4\gamma\kappa_C^{1-p}G\sec\theta(r_e\lambda_0)^2 T'_{C_kL}C_kL \qquad (5)$$

where C_kL is a commonly used parameter to measure the integrated strength of ionospheric turbulence [9, 10], γ is the ratio of the satellite velocity to the effective velocity of the IPP (so that $L_{SA} = \gamma L_C$), θ is the angle of incidence to the ionosphere from the satellite, $\kappa_C = 2\pi/L_C$, G is a geometric factor that is unity in an isotropic ionosphere [4, 5] and

$$T'_{C_kL} = \frac{\sqrt{\pi}\Gamma(p/2)}{(2\pi)^2\Gamma((p+1)/2)}\left(\frac{2\pi}{1000}\right)^{p+1} \qquad (6)$$

is a parameter that depends only on p [2]. In practice, the shape of the sidelobes can only normally be observed with a strong bright point target such as a corner reflector and are not immediately visible in an image of clutter.

1.4 Effect of the PSF on the radar clutter

The effect of ionospheric turbulence on a SAR image is largely described by the PSF and mainly takes place in the along track direction. The effect on the clutter statistics can be computed numerically by convolving an input undisturbed image with the ionosphere's PSF and then measuring the statistics of the output image. Since the PSF induced by the ionosphere is known [3], the effect on the statistics can also be derived analytically.

The complex ionospherically disturbed image $d(r)$ is given by the convolution with the PSF

$$d(r) = \frac{1}{\sqrt{\alpha_{TP}}} \int_{-\infty}^{\infty} u(r)h(r - \xi) \, d\xi \qquad (7)$$

where $u(r)$ is the complex undisturbed image, and only the ionosphere's effect in the along track direction is considered. The scaling factor $\alpha_{TP} = \int_{-\infty}^{\infty} |h(r)|^2 \, dr$ allows for the fact that the total power in the PSF may not be unity, and so ensures that power is conserved. Using (3)

$$d(r) = \frac{1}{\sqrt{\alpha_{TP}}} u(r) + \frac{1}{\sqrt{\alpha_{TP}}} \int_{-\infty}^{\infty} u(r)\mathrm{SLF}(r - \xi) \, d\xi \qquad (8)$$

where the mainlobe function (MLF) has been approximated to a delta function but with an attenuating scaling factor of α_{TP}. The PSF effectively removes power from the mainlobe (the undisturbed image) and puts it into the sidelobes.

The SLF is a random function [whose ensemble average is given by (4)] so that the effect of the ionosphere is to add random noise to each resolution cell of the undisturbed image, which for convenience will be referred to as ionospheric noise. Since this noise is determined by the local value of $u(r)$, to determine its effects on the image requires the assumption of a homogeneous area of stationary and ergodic statistics. Under this assumption, the convolution is equivalent to a stochastic integration over the product of $u(r)$ and $\mathrm{SLF}(r)$ rather than a convolution.

The amount of ionospheric noise added to each resolution cell is therefore given by

$$n_\sigma = \int_{-\infty}^{\infty} u(r)\mathrm{SLF}(r) \, dr \qquad (9)$$

In the absence of ionospheric effects, the PSF will be a delta function, that is, $h(r) = \delta(r)$ and consequently (8) reduces to $d(r) = u(r)$ since $n_\sigma = 0$.

2 Single point statistics

2.1 Introduction

In this section, the effect on the single point statistics is solved by first selecting an appropriate model of the clutter and then applying the ionospheric induced PSF. The resulting complex integral is then solved by calculating the probability of an intensity being observed for a constant background RCS and then determining the probability of that RCS. Finally, the probability of a given intensity is calculated and the moments and contrast determined.

2.2 Effect of ionospheric noise on clutter statistics

To determine the effect of the ionospheric noise, a statistical model of $u(r)$ is required. The complex image is usually modelled as the product of a slowly varying underlying cross section σ_0 with a zero mean complex Gaussian [11]. The Gaussian results in the familiar speckle noise that is a property of coherent imaging [12]. If the underlying cross section is gamma distributed, this compound model [11] results in a K-distributed amplitude and intensity with a phase uniformly distributed over 2π. This distribution is an excellent fit to nearly all non-urban measured data [13] and will therefore be assumed here. The complex image can

therefore be represented by

$$u(r) = \sqrt{\sigma_0(r)}\Big[\epsilon_R(r) + i\epsilon_Q(r)\Big]$$
$$= \sqrt{\sigma_0(r)\epsilon(r)} \qquad (10)$$

where $\sigma_0(r)$ is the RCS of the underlying terrain (which is assumed to have a constant mean μ and to be correlated over a correlation length of l_r resolution cells). The complex Gaussian $\epsilon(r)$ is assumed to be uncorrelated from one resolution cell to the next and causes speckle. Its components ϵ_R (real, in-phase) and ϵ_Q (imaginary, quadrature) are both zero mean Gaussians of variance $(1/2)$ so that $\langle |\epsilon(r)|^2 \rangle = 1$. The mean image intensity is therefore $\langle I \rangle = \langle |u(r)|^2 \rangle = \langle \sigma_0 \rangle = \mu$.

Each point in the SLF can be represented as a complex number $\eta(r)$ composed of two independent zero mean Gaussian random variables η_R and η_Q whose variance is determined by the envelope function $\langle |\mathrm{SLF}(r)|^2 \rangle$. The effect of the SLF on the disturbed image can therefore be written as

$$n_\sigma(r) = \int_{-\infty}^{\infty} \sqrt{\sigma_0(\xi)}\epsilon(\xi)\eta(\xi - r) \, d\xi \qquad (11)$$

This integral is a complex stochastic sum over a number of different independent random variables, each with different means, variances and indeed probability density functions (pdfs). As $\epsilon(r)$ is of zero mean and nominally unit intensity, the phase of $n_\sigma(r)$ is uniformly distributed over 2π, but the intensity pdf will depend on σ_0 as well. The underlying cross section σ_0 fluctuates slowly about its mean and is highly correlated from one resolution cell to the next. This suggests that the intensity pdf may be obtained by first determining the probability of intensity for a given constant σ_0, and then calculating the probability of that σ_0 occurring. The PSF will affect both of these terms, smoothing out the effective underlying cross-section variation and increasing the amount of Gaussian noise that manifests itself in the image as speckle.

Assuming stationary statistics, the effect of the complex Gaussian $\eta(r)$ may thus be determined separately to that of σ_0. The integration necessarily involves summation over many Gaussian components, so the sum of many values of $\eta(r)$ is equivalent to another Gaussian, but with a variance that is the sum of all the component variances. The variance of the single equivalent Gaussian is therefore

$$\sigma_{SLF}^2 = \int_{-\infty}^{\infty} |\eta(r)|^2 \, dr \qquad (12)$$

From (4) this integral over the SLF, provided that $p > 1$, is

$$\sigma_{SLF}^2 = T_{SLF} r_0^{1-p} \frac{\sqrt{\pi}\Gamma((p-1)/2)}{\Gamma(p/2)} \qquad (13)$$

Using (5) and (6), it can also be seen that σ_{SLF}^2 does not depend on the resolution and is directly proportional to $C_k L$

$$\sigma_{SLF}^2 = 4\pi\gamma G \sec\theta (r_e\lambda_0)^2 \frac{\Gamma((p-1)/2)}{\Gamma((p+1)/2)} 10^{-6} \left(\frac{l_0}{1000}\right)^{p-1} C_k L \qquad (14)$$

If the background $\sigma_0(r)$ is constant, the ionospheric noise

power, as given by its variance is $\sigma_n^2 = \sigma_0 \sigma_{SLF}^2$. It should be noted that this additive complex Gaussian noise is quite different to thermal noise [14] because it is directly proportional to the mean cross section and is therefore just as visible in regions of high RCS as low ones. It is also a measure of the loss of coherence and, since the mean power will be conserved between the disturbed and undisturbed images, must remove power from the mainlobe peak.

The intensity of this noise can therefore only be measured on a single image by exploiting inhomogeneity in the SAR image. A radar dark area, such as calm water or shadows that is adjacent to a much higher RCS background (such as forests) will therefore increase its RCS by σ_n^2 at the edge. The added noise can then be used to determine σ_{SLF}^2, which can be directly related to the strength of ionospheric turbulence. The main limitation of this method is that, it is strongly scene dependent and radar dark areas, such as shadows, are often not available. This is especially true as low frequency SAR tends to penetrate foliage, thus eliminating most shadows.

2.3 Probability of intensity I given σ_0

In the presence of ionospheric disturbance, zero mean complex Gaussian noise of variance σ_n^2 is added to each image pixel, but importantly the variance is proportional to the underlying cross section σ_0. It can therefore also be considered to be multiplied by the gamma distributed cross section. The ionospheric noise must therefore be combined with the Gaussian that causes the negatively exponentially distributed speckle i.e. $\epsilon(r)$. The variance of this new complex Gaussian is just the sum of the variances of its two components, so that the amplitude is Rayleigh distributed and the intensity pdf negatively exponentially distributed

$$p(I|\sigma_0) = \frac{1}{\sigma_0(1 + \sigma_{SLF}^2)} \exp\left\{-\frac{I}{\sigma_0(1 + \sigma_{SLF}^2)}\right\} \quad (15)$$

Thus the intensity of the speckle has increased for a given background cross section σ_0 as a result of the ionospheric disturbance.

2.4 Smoothing effect on $\sigma_0(r)$

In the previous sub-section, the effect of the ionosphere in terms of adding random Gaussian noise was considered, but unless the PSF induced by the ionosphere is a delta function, it will act to smooth the underlying cross section. This smoothing is described by the convolution of the underlying cross section with the PSF, so both the correlation lengths and the statistics of the underlying cross section must be considered. The underlying cross section σ_0 in the absence of ionospheric effects is generally considered to be gamma distributed [11, 13] with a pdf of

$$p(\sigma_0) = \frac{1}{\Gamma(v)}(b)^v \sigma_0^{v-1} \exp\{-b\sigma_0\} \quad (16)$$

where $b = v/\mu$. The order parameter v controls how 'spiky' the distribution is: as $v \to \infty$ the pdf becomes a delta function centred on the mean μ and the underlying terrain is constant and perfectly smooth. In the case of a disturbed ionosphere, the effective mean must be lower to conserve power and so

the ionospherically disturbed mean is $\mu_d = \mu/\alpha_{TP} = \mu/(1 + \sigma_{SLF}^2)$.

In practice, although the speckle is uncorrelated from one resolution cell to the next, the underlying terrain is often highly correlated. The nature of this correlation can only be fully described by the ACF $\rho_\sigma(r)$ of σ_0, but the simplest approach is to describe the correlation in terms of a correlation length l_r resolution cells beyond which a new independent sample of σ_0 is considered to occur. The characteristic function (Fourier transform of the pdf) of the gamma distribution is [15]

$$C_F(\omega) = (1 - i\omega\mu)^{-v} \quad (17)$$

Thus it can be seen that adding two independent gamma distributed random samples from the same underlying homogenous σ_0 does not change the mean but does double the order parameter. The convolution with the PSF therefore leaves the mean unchanged but increases the order parameter in direct proportion to the number of independent gamma distributed samples that are added together. The effective number of independent samples is therefore given by

$$\int_{-\infty}^{\infty} |\eta(r/l_r)|^2 \, dr = \frac{\sigma_{SLF}^2}{l_r} \quad (18)$$

The ionospherically disturbed order parameter is therefore given by

$$v_d = v(1 + \sigma_{SLF}^2/l_r) \quad (19)$$

The probability of observing cross section σ_0 in disturbed ionospheric conditions can therefore be approximated by the pdf

$$p(\sigma_0) = \frac{1}{\Gamma(v_d)}\left(\frac{v_d}{\mu_d}\right)^{v_d} \sigma_0^{v_d-1} \exp\left\{-\frac{v_d}{\mu_d}\sigma_0\right\} \quad (20)$$

The approximation here is that the PSF is equal to the ensemble average PSF, is spatially invariant, can be computed by adding intensities, and fully represents the effect on individual scatterers. In fact, none of these assumptions are strictly correct, since the PSF will vary randomly over the image, and the integration over the PSF is performed in amplitude and not intensity. However, the amplitude characteristic function does not have a closed-form solution, and adding intensities is equivalent to adding, and therefore conserving, the power. Furthermore, filtering the underlying cross section with the PSF does not represent the effect on individual scatterers. This is because they are not necessarily coherent over the synthetic aperture and filtering therefore changes the pdf [16]. However, the above approximation is reasonable, provided that the clutter coherence length does not change over the synthetic aperture, which will be the case provided that the PSF is not defocused. The errors in these approximations generally only manifest themselves in the higher order moments [12].

2.5 Probability density function

Using the compound model [11, 12], the intensity pdf is given by

$$p(I) = \int_0^\infty p(\sigma_0) p(I|\sigma_0) \, d\sigma_0 \qquad (21)$$

where $p(I|\sigma_0)$ is the probability of observing intensity I for a given cross section σ_0, and $p(\sigma_0)$ is the probability of observing cross section σ_0. Using the values derived in (15) and (20) results in the pdf

$$p(I) = \frac{2b_d}{\Gamma(v_d)} \left(\sqrt{b_d I}\right)^{v_{d-1}} K_{v_{d-1}}\left(2\sqrt{b_d I}\right) \qquad (22)$$

where $b_d = v_d/\mu$

The increase in the speckle intensity because of added ionospheric noise has been cancelled by the decrease in the effective underlying cross section (because of a reduced mainlobe height). Perhaps surprisingly, the result is a K-distribution of order v_d and unchanged mean intensity $\langle I \rangle = \mu$. The only significant change to the single point statistics is therefore the increase in the order parameter. Thus as the ionospheric turbulence increases, the underlying cross section (which constitutes the image) becomes smoothed out and the image dissolves into pure speckle.

2.6 Moments and contrast

The nth normalised moments of the K-distribution are [17]

$$I^{(n)} = \frac{\langle I^n \rangle}{\langle I \rangle^n} = n! \frac{\Gamma(n+v)}{v^n \Gamma(v)} \qquad (23)$$

As the ionospheric turbulence increases, the sidelobes increase and a loss of contrast occurs. Since the normalised second moment is $2(v+1)/v$ and the contrast is the standard deviation of intensity divided by the mean, the contrast is $\sqrt{I^{(2)} - 1} = \sqrt{1 + 2/v}$. The ratio of the disturbed image contrast to undisturbed contrast is therefore given by

$$\frac{c_d}{c_u} = \sqrt{\frac{v(v_d + 2)}{v_d(v+2)}} \qquad (24)$$

Thus when the order parameter v is already high, little loss of contrast occurs, whereas on a high contrast scene, the effects of the ionosphere will be much more visible. Provided that σ_{SLF}^2 is small, the contrast ratio is approximately

$$\frac{c_d}{c_u} \simeq 1 - \frac{\sigma_{SLF}^2/l_r}{2+v} \qquad (25)$$

As can be seen, although the ionospheric noise reduces the image contrast in proportion to the turbulence strength, it is not a particularly useful measure of the ionospheric state as it also depends on the order parameter. However, measuring the order parameter ratio and using (19) is a more useful measure of the ionospheric turbulence. This requires two SAR images of the same area, both generated from the same position in the orbit, but with one ionospherically disturbed and the other undisturbed. This situation often occurs in practice because most SARs orbit in a repeat cycle that generates identical ground tracks. The accuracy in

the estimate of v has already been determined [18] and can be used to derive the accuracy with which σ_{SLF} (and therefore $C_k L$) can be measured for a given v.

In practice, the observed higher order intensity moments are generally significantly less than those predicted above [12]. This is because the clutter is not fully coherent and is necessarily filtered by the imaging process [16]. The higher order moments do not therefore contain useable information about the ionosphere.

3 Two point statistics

3.1 Introduction

The two point statistics (also known as second-order statistics) of a SAR image are described by both the complex ACF and by the intensity ACF. The effect of the ionosphere's PSF on the complex ACF will be considered first, followed by the intensity ACF.

3.2 Complex ACF

The complex ACF, $\chi(X)$ is computed on the complex image and is given by

$$\chi(X) = \frac{\langle \varepsilon(x)\varepsilon^*(x+X) \rangle}{\langle |\varepsilon(x)|^2 \rangle} \qquad (26)$$

where $\varepsilon(x)$ represents the complex image (i.e. $d(x)$ or $u(x)$) in the along track x direction. This ACF may also be written in terms of the along track resolution cell r by dividing x by the resolution.

The averaging process implied by (26) can take place on a variety of scales. If it is assumed that the terrain cross section σ_0 is homogeneous (or at least varies slowly on a scale larger than the non-negligible part of the PSF) then, given that the complex field $\varepsilon(x)$ consists of clutter convolved with the PSF [12]

$$\chi(X) = \frac{\langle h(x)h^*(x+X) \rangle}{\langle |h(x)|^2 \rangle} \qquad (27)$$

As long as the averaging process takes place on a scale much larger than the clutter phase correlation length, the clutter averages out because its mean is zero. Any ionospheric process which results in uncorrelated additive noise, such as that from strong scattering from non-line of sight parts of the ionosphere, will also average out. Thus there is no requirement for the scattering to be weak for the complex ACF to take the form of (27).

The sidelobes of $h(x)$, which are also of random phase, will also average out provided that the averaging takes place on a scale larger than their correlation length. If the mainlobe amplitude (no sidelobes) is approximated as follows

$$|h(x)| = \exp\left\{-\frac{x^2}{w_x^2}\right\} \qquad (28)$$

where w_x is the half width of the mainlobe $1/e$ down from its peak (so that the 3 dB resolution is therefore $w_x\sqrt{2\ln 2}$), then in this case

$$\chi(X) = \exp\left[-\frac{X^2}{2w_x^2}\right] \qquad (29)$$

Any broadening of the mainlobe width w_x by an amplitude weighting $A(x)$ over the synthetic aperture will therefore manifest itself in a broadening of the complex ACF. Amplitude scintillation, which will modify $A(x)$, also produces zero mean but symmetrical sidelobes, and will not average out provided that the averaging takes place over an interval smaller than the Fresnel zone size. Any deviation of the complex ACF from the ACF of the mainlobe is therefore a symptom of ionospheric scintillation.

3.3 Intensity ACF

The along track ACF of image intensity $I(x)$ is given by Oliver and Quegan [19]

$$\frac{\langle I(x)I(x+X)\rangle}{\langle I(x)\rangle^2} = 1 + |\chi(X)|^2 + \iota_1(X) + \iota_2(X) \qquad (30)$$

where ι_1 and ι_2 are integrals that are zero for an underlying terrain with no structure (i.e. pure speckle and $v = \infty$). For such a terrain, (30) reduces to the Siegert relationship [20]. The forms of ι_1 and ι_2 have already been determined assuming that the PSF is translationally invariant [19]. Although this assumption is not normally valid for an ionospherically generated PSF, it is reasonable to assume that the ensemble average PSF will be a translationally invariant even function, and therefore the results will still hold, at least on average. Thus

$$\iota_1 = \int\int_{-\infty}^{\infty} \frac{\rho_\sigma(\xi_2 - \xi_1)}{v\alpha_{\text{TP}}^2}|h(\xi_1)|^2|h(\xi_2 - X)|^2 \, \mathrm{d}\xi_1 \, \mathrm{d}\xi_2 \quad (31)$$

where $\rho_\sigma(x)$ is the correlation function of the underlying terrain, and as before, α_{TP} is the total power in the PSF. If the terrain is a Markov random field, then the along track correlation function can be assumed to have the form [13]

$$\rho_\sigma(r) = \exp\left\{-2\frac{|r|}{l_r}\right\} \qquad (32)$$

with l_r being the $1/e$ correlation length in resolution cells. Although this form of the terrain correlation function is typical, it should be noted that it can have any form and is a property of the terrain, not the imaging process.

If $h(x)$ is a delta like function, the ι_1 integral reduces to

$$\iota_1 \simeq \frac{\rho_\sigma(X)}{v} \qquad (33)$$

In practice, since $h(x)$ is not a delta function, the PSF will act to smooth out any rapid variations in ρ_σ, but since this is usually a slowly varying function, little effect will be observed and (33) is a good approximation.

For the form of ρ_σ given in (32) above, the integral ι_1 can be solved if $/h(\xi_1)|^2$ in the integral is approximated to a delta function and the SLF of (4) is assumed. The integral becomes a convolution between the PSF and the terrain correlation function (as was assumed for the single point statistics) and the same result as in (33) is obtained, but with v replaced by v_d. The slope of $\rho_\sigma(r)$ as a function of resolution cell r is therefore largely unaffected by the ionosphere.

The second integral in (30), also assuming that $h(x)$ is an even function, is [19]

$$\iota_2 = \int\int_{-\infty}^{\infty} \frac{\rho_\sigma(\xi_2 - \xi_1)}{v\alpha_{\text{TP}}^2}h(\xi_1)h(\xi_1 - X)h^*(\xi_2)h^*(\xi_2 - X) \, \mathrm{d}\xi_1 \, \mathrm{d}\xi_2 \qquad (34)$$

Again, if it is assumed that $h(x)$ is a delta like function, this integral reduces to

$$\iota_2 \simeq \frac{\rho_\sigma(0)}{v}\frac{|h(X)|^2}{\alpha_{\text{TP}}} \qquad (35)$$

The presence of $|h(X)|$ in this expression is an approximation, but it illustrates that were it not for the double integral and the more dominant terrain correlation term ι_1, the intensity ACF would have a direct dependence on the SLF. The integral ι_2 is normally only significant near the peak of the ACF where $X \simeq 0$ and $\iota_2 \simeq 1/v$. Away from that part of the intensity ACF where $|\chi(X)|^2$ dominates, the ACF is largely unaffected by the ionosphere, since the terrain correlation ρ_σ dominates and is a slowly varying function. The intensity ACF therefore remains a good measure of the correlation length l_r, even under ionospheric disturbance.

At the zero point (i.e. $X = 0$) the intensity ACF peak is $2 + 2/v$ and can therefore also be used to measure the order parameter. This result is to be expected since by definition the zero point of the ACF is the normalised second moment, as given in (23). The peak of the intensity ACF should therefore decline under disturbed ionospheric conditions since the order parameter will rise.

3.4 Theory: conclusions

The effect of the ionosphere on a SAR image is measureable in a number of ways, even when it does not result in defocusing. The most important of these are the rise in the order parameter in direct proportion to the strength of turbulence. The complex ACF is primarily a measure of the mainlobe, but by exploiting difference in the correlation distances of sidelobes, some indication of amplitude scintillation can be obtained. The intensity ACF allows the correlation distance of the underlying terrain to be measured, as well as the order parameter. The turbulence slope p, and outer scale l_0, cannot be determined using these measures.

In practice, it is difficult to measure the ionosphere from the clutter given only one image because it is not possible to distinguish between terrain effects and ionospheric effects. Although assumed prior knowledge could be used, the best form of prior knowledge is to compare two SAR images of the same area. Since most satellites orbit along the same ground tracks repeatedly (often for sun synchronous reasons or to allow repeat-pass interferometry) there is a great deal of imagery for which comparison can be made. This approach does not of course work over the sea, which changes its statistical properties with the prevailing tropospheric weather.

4 Simulation

4.1 Introduction

As is well known, it is particularly difficult to simulate K-distributed clutter with both the correct ACF and single

point statistics [13, 15]. However, the ionospherically induced PSF as given by (4) may be applied to undisturbed data obtained from a SAR (such as PALSAR [21]) relatively easily. It can also be applied to SAR data simulated using (10), although the ACF will not necessarily be realistic.

This provides a partial test of the assumptions made in deriving the change in the order parameter as a result of propagation through the ionosphere. It is not though a full test because it assumes that the effect of the ionosphere is fully represented by the PSF, whereas in fact not only will the PSF exhibit temporal and spatial variations over the synthetic aperture, but the effect on each individual scatterer cannot be properly described by a PSF in any case.

A simulation was performed by first selecting an image from an undisturbed PALSAR scene that was homogeneous and reasonably large (2175×1024 pixels). An area of continuous Brazilian rainforest of relatively high RCS, about -11 dBm^2/m^2 was selected to avoid the systematic bias in the estimate of v that can occur at low values of v and low signal-to-noise ratios [22, 23]. A randomly generated PSF was then applied to each range gate and the resulting order parameter measured. In reality, the PSF would be highly correlated in the range direction (at least on a scale of the Fresnel zone) and would change along track. The simulation therefore only tests the relationship between the order parameter and the PSF as given by (14) and (19).

The PSF was simulated assuming an isotropic ionosphere half way between the satellite and the ground (so $\gamma = 2$) and an outer scale $l_0 = 10$ km. The order parameter itself was measured on the single point statistics using the natural log-method of Blacknell and Tough [18]

$$v = \left[\frac{\langle I \log I \rangle}{\langle I \rangle} - \langle \log I \rangle - 1 \right]^{-1} \qquad (36)$$

4.2 Simulation results

The result of the simulation is shown in Fig. 1, from which it can be seen that there is a noise floor at about -20 dB. This level was only achieved by virtue of using large images and is probably unachievable in practice. As the value of $C_k L$ rises, so too does the order parameter in a manner broadly consistent with the theory. Once the value of $C_k L$ reaches the level at which defocus occurs, the theory breaks down and the order parameter no longer rises with increasing $C_k L$. Little can be read into the decline in the order parameter ratio after defocusing because the simulation relies on the form of $h(x)$ as given in (3) being correct, which it is not under defocus.

The value of p determines the sidelobe roll off rate of the PSF, so the lower the value of p, the slower the roll off rate and thus more energy can appear in the sidelobes before a defocus occurs. The value of the order parameter can, therefore be much higher for small value of p, which is as observed in Fig. 1. The value of the ionosphere's outer scale size, l_0, cannot be derived from the imagery, but does affect the slope of the lines in Fig. 1 because it affects how much energy can appear in the sidelobes for a given $C_k L$. When l_0 is less than the synthetic aperture L_{SA}, more energy can appear in the sidelobes before defocus, so the order parameter ratio can rise further.

Substituting the homogeneous PALSAR image used as the basis for simulation with another inhomogeneous image (with a river running through it) produces similar results to those in
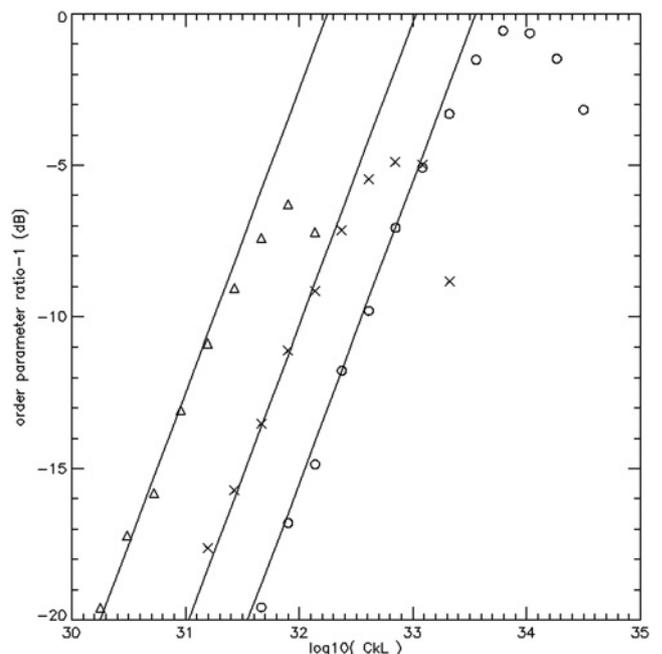

Fig. 1 *Simulated order parameter ratio as a function of $log_{10}(C_k L)$ for $p = 1.5$ (o) $p = 2.5$ (x) and $p = 3.5$ (Δ) together with a fit to the theory (solid lines)*

Fig. 1, suggesting that the order parameter ratio is a robust measure of ionospheric scintillation. Furthermore, simulating the clutter using (10) produces much the same result, suggesting that the ACF is not critical, and indeed for all the simulation performed here, the effective $l_r = 1$.

4.3 Simulation conclusions

The simulation clearly demonstrates that it is possible to measure the effects of ionospheric scintillation on the clutter order parameter two orders of magnitude below the point where image defocusing occurs. In this simulation, the same image (before and after applying the PSFs) was used to measure the order parameter, but in practice a different realisation of the real clutter will occur on each satellite imaging pass. The statistical stability of the real clutter will therefore determine the accuracy of the order parameter measurement and how useful a quantity the order parameter ratio is for real imagery. Although there has been considerable previous work on optimal methods for estimating the K-distribution order parameter [18, 22, 23] there has been little work establishing how stable the clutter order parameter is on a daily or seasonal basis. The anisotropy of the ionosphere also limits the technique, since, if uncorrected, amplitude modulation in the range direction will actually result in a decrease in the order parameter ratio rather than an increase because of the higher variance.

5 Conclusions

The effect of the ionosphere on the SAR clutter statistics cannot be detected if there is no variation in the terrain, which in practice means that the effect is undetectable when either the surface correlation length is long or the order parameter very high. When this is not the case, the ionospheric turbulence increases the K-distribution order parameter v by a factor that is directly proportional to $C_k L$.

There is little effect on the intensity ACF (except for the increase in v) but this does allow the terrain correlation length to be measured. The complex ACF is affected by the ionosphere because the correlation distances in the ionosphere are longer than those in the clutter, which averages out, thus leaving only scintillation effects. The ionospheric spectral slope p and outer scale l_0 cannot be determined from the effect on the clutter, but since they affect the shape of the sidelobes, could be measured on a point target.

Since the effect of the ionosphere is to increase the order parameter, measuring the order parameter ratio between identical pairs of SAR images is a good measure of the change in ionospheric turbulence. At L-band the ratio is usually a direct measure of C_kL because the turbulence in one image of the pair can normally be approximated to zero. The order parameter ratio is therefore an important new measure of ionospheric turbulence.

The simulation clearly shows that it is possible to detect the effects of the ionosphere, as quantified by C_kL, two orders of magnitude lower than that required to cause defocusing. The technique clearly needs to be tested on real experimental data and two images with little temporal separation and a small order parameter are likely to produce the best results. The experimental stability of the order parameter in the absence of ionospheric effects is unknown, but its statistical stability is likely to be correlated with the interferometric coherence.

6 Acknowledgments

7 References

1 Belcher, D.P.: 'Theoretical limits on SAR imposed by the ionosphere', *IET Proc. Radar, Sonar Navig.*, 2008, **2**, (6), pp. 435–448, doi:10.1049/iet-rsn:20070188

2 Belcher, D.P.: 'Sidelobe prediction in transionospheric SAR imaging radar from the ionospheric turbulence strength CkL'. Proc. Radar 2008 Conf., Adelaide, Australia, 3-5 September 2008, doi:10.1109/RADAR.2008.4653891

3 Belcher, D.P., Rogers, N.C.: 'Theory and simulation of ionospheric effects on SAR', *IET Proc. Radar, Sonar Navig.*, 2009, **3**, (5), pp. 541–551, doi:10.1049/iet-rsn.2008.0205

4 Rino, C.L.: 'A power law phase screen model for ionospheric scintillation, 1 weak scatter', *Radio Sci.*, 1979, **14**, (6), pp. 1135–1145

5 Rino, C.L.: 'On the application of phase screen models to the interpretation of ionospheric scintillation data', *Radio Sci.*, 1982, **17**, (4), pp. 855–867

6 Yeh, K.C., Liu, C.H.: 'Radiowave scintillation in the Ionosphere', *Proc. IEEE*, 1982, **70**, (4), pp. 324–360

7 Fremouw, E.J., Livingston, R.C., Miller, D.A.: 'On the statistics of scintillating signals', *J. Atmos. Solar Terr. Phys.*, 1980, **42**, pp. 717–731

8 Harris, F.J.: 'On the use of windows for harmonic analysis with the discrete Fourier transform', *Proc. IEEE*, 1978, **66**, (1), pp. 51–83

9 Secan, J.A.: 'WBMOD ionospheric scintillation model—An abbreviated user's guide V13' (NorthWest Research Associates, Bellevue, Washington, USA, 1996)

10 Secan, J.A., Bussey, R.M., Fremouw, E.J., Basu, S.: 'An improved model of equatorial scintillation', *Radio Sci.*, 1995, **30**, pp. 607–617

11 Ward, K.D.: 'Compound representation of high resolution sea clutter', *Electron. Lett.*, 1981, **17**, pp. 561–565

12 Oliver, C.J.: 'Information from SAR imges', *J. Phys. D. Appl. Phys.*, 1991, **24**, pp. 1493–1514

13 Oliver, C.J.: 'The interpretation and simulation of clutter textures in coherent images', *Inverse Problems (IoP)*, 1986, **2**, pp. 481–518

14 Watts, S.: 'Radar detection prediction in K-distributed sea clutter and thermal noise', *IEEE Trans. Areosp. Electron. Sys.*, 1987, **AES-23**, (1), pp. 40–45

15 Blacknell, D.: 'New method for the simulation of correlated K distributed clutter', *IEE Proc. Radar, Sonar Navig.*, 1994, **141**, (1), pp. 53–58

16 Oliver, C.J.: 'A model for non-Rayleigh scattering statistics', *Opt. Acta (now called J. Mod. Opt.)*, 1984, **31**, (6), pp. 701–722

17 Jakeman, E.: 'On K distribution noise', *J. Phys. A: Math Gen.*, 1980, **13**, pp. 31–48

18 Blacknell, D., Tough, R.J.A.: 'Parameter estimation for the K-distribution based on [z log(z)]', *IEE Proc. – Radar, Sonar Navig.*, 2001, **148**, (6), pp. 309–312, doi:10.1049/ip-rsn:20010720

19 Oliver, C.J., Quegan, S.: 'Understanding synthetic aperture radar images' (Artech House, 1998), section 5.6, ISBN 089006850X

20 Siegert, A.J.F.: 'Report no. 465', MIT Rad. Lab., 1943

21 Rosenqvist, A., Shimada, M., Ito, N., Watanabe, M.: 'ALOS PALSAR: a pathfinder mission for global-scale monitoring of the environment', *IEEE Trans. Geosci. Remote Sens.*, 2007, **45**, (11), pp. 3307–3316, doi:10.1109/TGRS.2007.901027

22 Lomardo, P., Oliver, C.J., Tough, R.J.A.: 'The effect of noise on order parameter estimation for K distributed clutter', *IET Proc. Radar, Sonar Navig.*, 1995, **142**, (1), pp. 33–40

23 Lombardo, P., Oliver, C.J.: 'Estimation of texture parameters in K distributed clutter', *IEE Proc. Radar, Sonar Navig.*, 1994, **141**, (4), pp. 196–204